Journal of Archaeological Science 40 (2013) 1108–1121

Contents lists available at SciVerse ScienceDirect

Journal of Archaeological Science

journal homepage: http://www.elsevier.com/locate/jas

Towards a three-dimensional cost-effective registration of the archaeological heritage

Jeroen De Reu [a,*], Gertjan Plets [a], Geert Verhoeven [a], Philippe De Smedt [b], Machteld Bats [a], Bart Cherretté [c], Wouter De Maeyer [c], Jasper Deconynck [d], Davy Herremans [a], Pieter Laloo [d], Marc Van Meirvenne [b], Wim De Clercq [a]

[a] *Department of Archaeology, Ghent University, Sint-Pietersnieuwstraat 35, B-9000 Ghent, Belgium*
[b] *Research Group Soil Spatial Inventory Techniques, Dept. of Soil Management, Ghent University, Coupure 653, B-9000 Ghent, Belgium*
[c] *SOLVA, Zuid III, Industrielaan 18, B-9320 Aalst (Erembodegem), Belgium*
[d] *GATE bvba, Eindeken 18, B-9940 Evergem, Belgium*

ARTICLE INFO

Article history:
Received 19 May 2012
Received in revised form
22 August 2012
Accepted 23 August 2012

Keywords:
Three-dimensional registration
Archaeological heritage
Excavations
Agisoft PhotoScan
Computer vision
Structure from motion

ABSTRACT

Archaeological practice within the European context of heritage management is facing huge challenges in ways of recording and reproduction of ex-situ preserved sites. As a consequence of the Valletta-treaty, numbers of archived images and drawings of excavated structures as prime sources of past human activity, are exponentially growing. Contrarily to portable remains however, their future study and revision is biased by the two-dimensional character of the recorded data, rendering difficult their future reconstruction for new study or public dissemination. A more realistic three-dimensional (3D) way of recording and archiving should be pursued. In this paper the possibilities for 3D registration of archaeological features are examined in a computer vision-based approach using the PhotoScan software package (Agisoft LCC). It proved to be a scientific and cost-effective improvement compared to traditional documentation methods. Advantages can be found in the high accuracy and straightforwardness of the methodology. The extraction of an orthophoto or a Digital Terrain Model from the 3D model makes it feasible to integrate detailed and accurate information into the digital archaeological excavation plan. The visual character of 3D surface modeling offers enhanced output-possibilities allowing a better documentation of in-situ structures for future research and a higher public participation and awareness for the archaeological heritage.

1. Introduction

1.1. Context and aims

Archaeological remains constitute a considerable part of the cultural heritage. Investigating the past by means of excavations can be considered in many cases as a process of guided destruction of the excavated heritage itself, especially when no stone structures are involved or when no preservative measures are taken. This creates a fundamental epistemological paradox: the production of scientific historical knowledge by means of excavations directly leads to the very destruction of its basic *in-situ* dataset, rendering reproduction of the data and a future revised scientific and public interpretation potentially problematic.

Portable material culture finds, although extracted from their in-situ positions and preserved in heritage collections and depots, are most often the only remaining original data-source allowing future new studies and interpretations. However, the contexts from which they were divorced during excavation are mostly not preserved. These principal witnesses of past human activity are only preserved *ex-situ* by means of contemporary-produced evidence such as drawings, photographs and – in a very few cases – films which generates a loss of information and renders them less suitable for later study and revisions. Consequently, the present and future scientific and public community are basically left with a two-dimensional interpretation of a 3D structural dataset from heritage remains recorded in the field.

This problem has never been more apparent than it is today. Since the ratification or application of the guiding principles of the Valletta Treaty,[1] in many European countries, archaeological research has undergone fundamental changes (Kristiansen, 2009).

* Corresponding author. Tel.: +32 93310155.
E-mail address: Jeroen.DeReu@UGent.be (J. De Reu).

[1] Convention on the Protection of the Archaeological heritage of Europe, also known as Malta Convention: http://conventions.coe.int/Treaty/en/Treaties/Html/143.htm

0305-4403/$ – see front matter © 2012 Elsevier Ltd. All rights reserved.
http://dx.doi.org/10.1016/j.jas.2012.08.040

One of the consequences is an exponentially growing set of two-dimensional data, produced by a continuously increasing number of archaeological researches on terrains potentially threatened by infrastructural works. For the Flemish archaeology for instance, this is well illustrated by the number of excavation permits issued, rising with 453% between 2004 and 2009 (De Clercq et al., 2012). Another fundamental change can be observed in practices of evaluation and excavation. These must be adapted to several evolving scientific, economic and social parameters such as large scale excavations, assessment of quality and preservation, restraints in time and money, technological evolution and the need to increase public awareness. As a consequence the processes of registration of the archaeological heritage have become increasingly digitized, mostly in order to speed up the work-flow and output. However, the basic documentation from the excavated contexts, albeit digitized, still provides present and future communities with a large dataset biased by interpretation (drawing) and a two-dimensional view.

Archaeological investigations require detailed, high resolution registration and documentation techniques, in order to maximize the opportunities for future reproduction of the structural dataset, especially when it comes down to remains from non-preserved or non-stone build sites such as soil-features and structures in organic material. In the framework of contemporary archaeological heritage management, these methods should be fast and accurate, easily accessible and manageable for contemporary and future communities and preferably proceeding to a more than two-dimensional way of data-storage and reproduction of the structural components from the archaeological heritage. Multi-dimensional recording and reproduction of excavated structures could potentially bridge the gap between *in* and *ex-situ* preservation. It could enhance the quality of the archived heritage for future perception and study by offering a better visualization and allowing a personal participation of the present and future data-viewers in the manipulation of the images of the excavated structures.

This paper aims therefore at investigating the possibilities of a low-cost computer vision-based software package, Agisoft PhotoScan (AgiSoft LLC, 2011b), for the 3D documentation of archaeological research using ordinary overlapping images. Based on case-studies developed in the framework of Flemish archaeological heritage management as well as in scientific research, 3D surface modeling is investigated as a method for (i) the registration of archaeological surfaces and contexts during excavations, (ii) the visualization of excavation data during the post-excavation process and (iii) the visualization of the unmovable archaeological heritage for a professional and a wider audience.

1.2. A review of 3D techniques applied in archaeological field recording

In the last decade, 3D applications have increasingly found their way into archaeological heritage research. Several studies focused on the registration and preservation of rock art, with examples on the British Isles (Chandler et al., 2007; Simpson et al., 2004), the Iberian Peninsula (Lerma et al., 2010; Sanz et al., 2010), Australia (Chandler et al., 2005, 2007) and in the Altai Mountains, Russia (Plets et al., 2012a, 2012b) or the registration and preservation of ancient temples and monuments (e.g. Al-kheder et al., 2009; Barazzetti et al., 2011; Grün et al., 2004; Karauğuz et al., 2009; Rajani et al., 2009) and even dinosaur footprints (Remondino et al., 2010). Other studies implemented 3D in the analysis of archaeological artifacts, including lithics (e.g. Clarkson and Hiscock, 2011; Lin et al., 2010), pottery (e.g. Karasik and Smilansky, 2008; Koutsoudis et al., 2009, 2010; Koutsoudis and Chamzas, 2011; Tsiafakis et al., 2004; Zapassky et al., 2006) and faunal remains (e.g. Niven et al., 2009). Furthermore, 3D technologies are frequently used in the reconstruction (e.g. Fatuzzo et al., 2011; Rua and Alvito, 2011) and the presentation (e.g. Bruno et al., 2010; Chow and Chan, 2009; Plets et al., 2012b; Tsiafakis et al., 2004) of the archaeological heritage. Although the application of 3D technology in archaeological surveys and excavations remains rather limited, these techniques are becoming more and more prevalent in archaeological fieldwork. Several researchers have combined GPS or Total Station field recordings with 3D GIS to obtain 3D excavation plans (e.g. Barceló et al., 2003; Barceló and Vicente, 2004; Katsianis et al., 2008; Losier et al., 2007), while other researchers have investigated laser scanning for the recording of archaeological excavations (e.g. Doneus and Neubauer, 2005; McPherron et al., 2009). Tokmakidis and Skarlatos (2002) have used close ranged photogrammetry to produce an orthophoto and Digital Terrain Model (DTM) of an archaeological excavation. Finally, Pollefeys et al. (2000), (2003); Doneus et al. (2011), Verhoeven (2011) and Verhoeven et al. (2012), (in press) have applied computer vision techniques for the 3D registration of archaeological sites and excavations and/or archaeological landscapes.

Recent technical advances in 3D recording illustrated the potential for 3D registration in archaeological and cultural heritage studies (Pavlidis et al., 2007). These techniques, as described in detail by Remondino and El-Hakim (2006), are based on (i) image-based modeling, including photogrammetry (e.g. Guidi et al., 2004; Hendrickx et al., 2011; Koutsoudis et al., 2007), (ii) range-based modeling (e.g. Entwistle et al., 2009; Fowles et al., 2003; Lerones et al., 2010; Lin et al., 2010; Stojakovic and Tepavcevic, 2011) or (iii) a combination of image-based and range-based modeling (e.g. Al-kheder et al., 2009; Lambers et al., 2007; Lerma et al., 2010; Yastikli, 2007). However, both methods require a certain degree of expertise and are not straightforward implementable during archaeological fieldwork. Furthermore, aiming at both a scientific and cost-effective improvement of the archaeological documentation methods, these techniques are often time consuming and can be rather expensive. From the cost-effective point of view, the recent developments in computer vision, aiming at developing mathematical techniques for recovering the 3D shape and appearance of objects in imagery (Szeliski, 2011: 3), are promising. The implementation of various computer vision techniques such as structure from motion (SfM) and dense stereo-reconstruction algorithms in low-cost or open source computer vision based software packages (e.g. Autodesk 123D Catch (Autodesk Inc., 2012), Automatic Reconstruction Conduit (ARC 3D) (VISICS, 2011), Bundler (Snavely, 2010), PhotoModeler Scanner (Eos Systems Inc., 2012), PhotoScan (AgiSoft LLC, 2011b), Photosynth (Microsoft Corporation, 2011) or VisualSFM (Wu, 2012)), makes the generation of 3D point clouds and representations easy accessible, even for users without an intimate technical background.

2. Method

For the 3D registration of the archaeological heritage, the low-cost software package PhotoScan (professional edition), released mid-2010 by the Russian manufacturer AgiSoft LCC, was applied (AgiSoft LLC, 2011b). It allows the extraction of 3D data from ordinary 2D images using SfM and dense stereo-matching algorithms. The workflow presented is inherent to the characteristics of PhotoScan and consists of two general steps, data collection and data processing.

2.1. Data collection

The data acquisition is the only phase of the process taking place in the field. It comprises two steps, (i) the recording of ground control points or reference distances and (ii) the imaging of the scene. The latter is executed by acquiring conventional photographs from the scene, taken with uncalibrated cameras and lenses. Since the resulting 3D model is always computed in a local coordinate framework with relative dimensions, one needs to include additional information to extract absolute metrical information from the model. On the one hand, ground control points (GCPs) can be included to achieve an absolute 3D georeferencing. On the other hand, reference distances between well-indicated points allow the model to be scaled in an absolute way, so that accurate measurements also become possible. In cases where one opts for the first method, a DTM of the object under study can be produced as well. In two of the presented case studies the GCPs were recorded using a Trimble G6 D-GPS with differential corrective. In the third case a total station was used to measure the GCPs, while in the last case study reference distances were used.

When the GCPs are set, the image acquisition can start. The photographs need to be taken, preferably from unique viewpoints with sufficient overlap (AgiSoft LLC, 2011a). A first image collection captured the object as globally as possible, after which more close-range imagery was added to provide the necessary detail. Pictures from above were taken by mounting the camera on a tripod. At two sites the images were shot using a 12.1 megapixel Nikon D700 FX reflex camera equipped with a 24–70 mm f/2.8G ED AF-S NIKKOR objective. At the other two sites the images were collected with a consumer grade Olympus digital camera, respectively the Olympus μTough-8010 (14.0 megapixel) and the Olympus μ-1030 SW (10.1 megapixel).

2.2. Data processing

Using PhotoScan, a 3D model can be generated in a fully automated three-step process (AgiSoft LLC, 2011a; Verhoeven, 2011), comprising (i) the alignment of the photographs, (ii) the calculation of a dense 3D surface and finally (iii) the texture mapping of the model. However, it is possible to intervene in the process at any stage.

Before starting with the alignment of the photos and the processing of a 3D model, a pre-processing of the implemented photographs is recommended, as the results largely depend on the quality of the imagery. Therefore it is useful, however not obligatory, to mask those areas in the images where "moving objects" (e.g. shadows or displaced objects) occur, where information about the texture of objects is lacking (e.g. sky and shiny objects) or where the variation in texture is little (e.g. full white objects) (Fig. 1). Photographs that only depict zones without texture or "moving

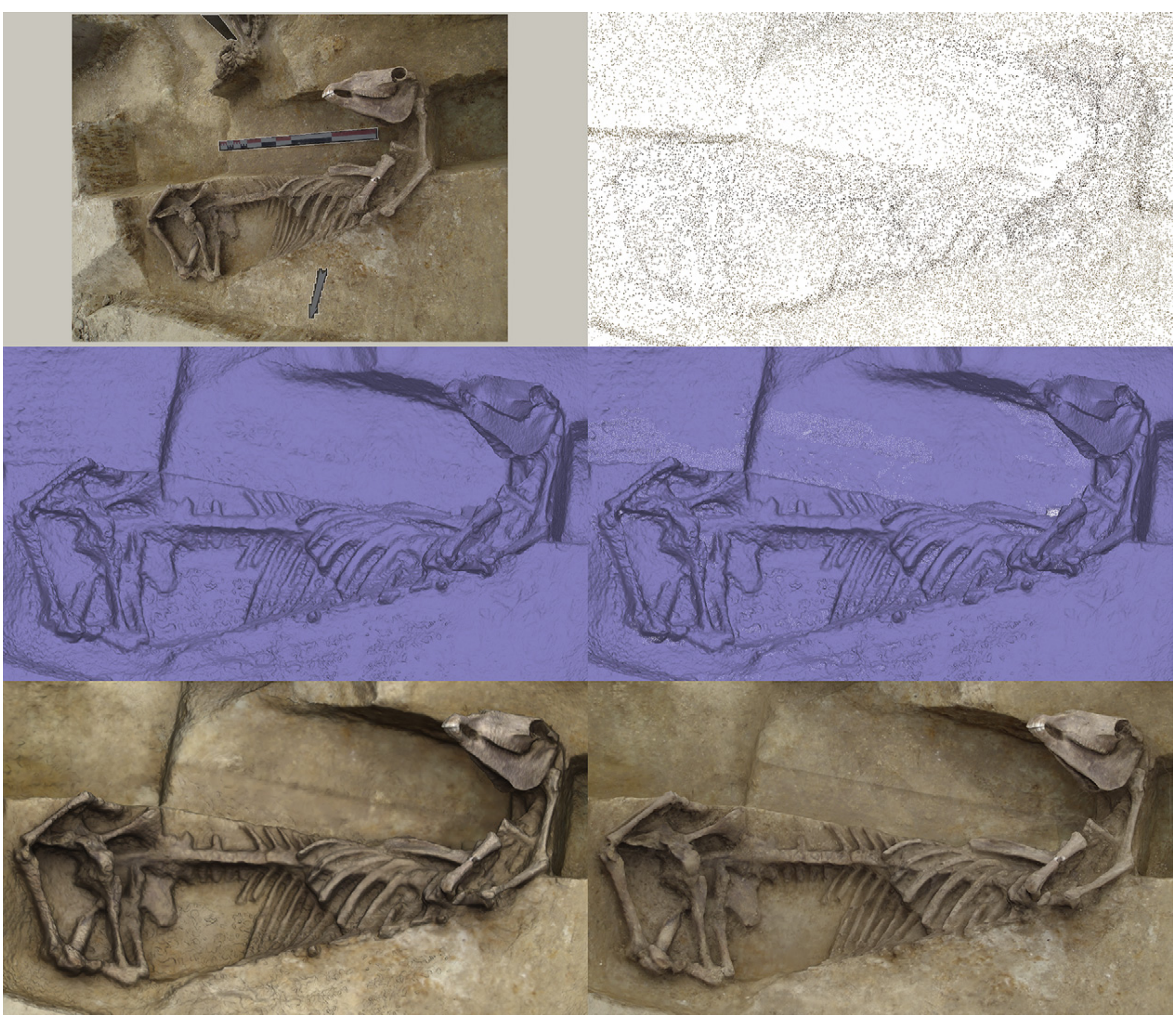

Fig. 1. Several phases in the 3D surface modeling: a photograph with masked areas (top left); a 3D sparse point cloud (top right); a polygonal mesh visualized in shaded (middle left), wireframe (middle right) and solid mode (bottom left); mapped texture on a 3D geometric surface (bottom right).

objects" can simply be omitted. The enabling, disabling or masking of (parts of) photographs can be adjusted at any stage of the process.

After the treatment, the processing of the 3D model starts by aligning the photographs. During this step (i) a 3D sparse point cloud is generated representing the geometry of the scene (Fig. 1), (ii) the relative orientation of camera position at the moment of image acquisition is determined and (iii) the internal camera parameters (focal length, principal point location, skew, radial and tangential distortion coefficients) are computed. For the processing of the alignment, PhotoScan uses a structure from motion approach (SFM; (Ullman, 1979), see also (Szeliski, 2011)). This step largely determines the final accuracy of the 3D model, so it is useful to visually check the image alignment and the computed projection error after the computations.

During the second step, the computationally most intensive operation in the processing, the 3D geometry (i.e. the surface) of the model is built (Fig. 1). Therefore, the software uses dense, multi-view stereo-matching algorithms (e.g. Scharstein and Szeliski, 2002; Seitz et al., 2006). The computation time largely depends on the resolution and the quantity of the used imagery and the level of detail wanted in the geometric model. The output is a polygonal mesh, visualized in a solid, shaded and wireframe mode (Fig. 1). Besides the computation of the 3D geometry, this second step also calculates the color for each model vertex and stores it as an attribute. During the rendering of the model, these colors (which are an average of the corresponding pixel values from the source photos) are then interpolated for each polygon face, so that each face of the model is filled by a color gradient. When the number of polygons is large, this vertex color approach already provides a very good visual representation of the objects surface (Fig. 1). The processing time required for the generation of a polygonal mesh in the presented case studies took around 12–24 h. The data processing was performed using a Dell™ Precision™ T7500 with One Intel® Xeon® X5680 (3.33 GHz, 6.4 GT/s, 12 MB, 6C) processor, 24 GB DDR3 1333 MHz ECC-RDIMM (6×4 GB) memory, a 64-bit operating system (Windows 7) and a 2 GB GDDR5 ATI FirePro V7800 graphic card.

When even better textures are needed, it is possible to apply a separate texture mapping. This step calculates a so-called texture atlas out of one or more source photographs. Each model vertex now stores its coordinate in this texture atlas. During rendering of the 3D object, these coordinates are used to map the texture image onto the 3D model surface (Fig. 1). Since the original photographs are mapped onto the geometrical surface, this step makes it possible to provide a very rich texture for each polygon in the model. Although this step is not necessary for the output of a DTM or orthophotograph, it comes in handy when only a textured 3D model is needed as output (e.g. as starting point in a 3D animation program). Moreover, a texture image with adequate resolution to visualize the details can significantly help in the subsequent indication of the reference points.

After the processing of the 3D model, some post-processing actions are recommended depending on the final use of the model. The transformation of the reconstruction into an absolute coordinate frame is required for the generation of DTMs and the calculation of distances, volumes and surface areas. This can be done by using reference coordinates or partially by reference distances. When using coordinates, either GCP coordinates or coordinates of the camera positions can be used. In this paper, only GCPs were applied to derive the absolute orientation of the 3D model. At least three GCPs are required with known *x*-, *y*-, and *z*-coordinates. By using reference distances, the 3D model is not georeferenced but absolutely scaled, which also allows the extraction of metric information (e.g. surface area, volume). Both procedures also enable an assessment of the accuracy of the generated model.

Even though a 3D model is a scientifically valid means of documentation and presentation, it requires special software to view. When printed on a 2D sheet of paper, it loses all its geometrical value. To remedy this, an orthophoto of the 3D model can be created. This orthophoto offers a geometrically correct image in which all possible deformations, due to camera tilt and variations in object height, are corrected. As such, accurate metric measurements can be made in a 2D environment. Finally, PhotoScan also supports the export of a DTM, a point cloud or the 3D model itself (i.e. OBJ, 3DS, WRL, DAE, PLY, DXF, U3D or PDF file format).

3. Results

The 3D registration of archaeological heritage using the PhotoScan software was investigated on three excavations, including both rural and urban contexts dating from the Roman and Medieval period, conducted during the summer of 2011. The selected contexts inquire a lot of time for manual registration due to their complexity and include foundations, a cellar and a well. A fourth case study, subjecting two horse skeletons, investigates the possibilities of using "old" imagery of past excavations for 3D surface modeling.

3.1. Foundations of an outbuilding at the abbey site of Boudelo

Recently, an electromagnetic induction survey (EMI) revealed a complex designed Medieval landscape consisting of numerous ditches, moated sites and outlines of architectural constructions, south of the during the 1980's excavated cloister range of the Cistercian abbey of Boudelo (Stekene, prov. East Flanders, Fig. 2) (De Smedt et al., 2011). A limited excavation (160 m^2) was conducted by Ghent University in order to further interpret the detected structures and to evaluate the site for in-situ preservation and conservation of the remaining archaeological heritage of the abbey. The evaluation trench confirmed the presence of a moated site with two large ditches as part of a larger enclosure system. On the island, a large and presumably wooden structure was built on dadoes (i.e. foundations) in local brick. The analyzed structures can be interpreted as part of the economic centre of the Cistercian house during the late 13th and early 14th century. Two dadoes were selected for 3D registration. The images were taken with the previously described Nikon equipment.

The first dado was documented with 40 photographs, taken from unique viewpoints around and above the scene (Fig. 3). Using the Agisoft PhotoScan software a 3D point cloud, containing 475,000 points and a polygonal mesh, consisting of 8.1 million faces and 4.1 million vertices, were generated. The absolute georeferencing of the resulting surface model was performed with the manual identification of 14 GCPs recorded in the field. The longest diagonal between two GCPs is 2.406 m. The difference in height between the highest and lowest GCP is 0.320 m. The total RMSE (root mean square error) of the model reported between the computed coordinates and the GCP values is 0.015 m and the individual RMSE for the *x*-, *y*- and *z*-axis measure respectively 0.006, 0.009 and 0.011 m (Table 1). On a 1:10, 1:20 and 1:50 scale this error corresponds to a distance of respectively 1.50 mm, 0.75 mm and 0.30 mm, representing an accuracy which can hardly be obtained when manually documenting in the field. Although these metrics only give an idea about the georeferencing quality and do not really assess the true vertical and horizontal positional accuracy of the complete 3D model, the low georeferencing errors do, however, indicate that no large systematic distortions are

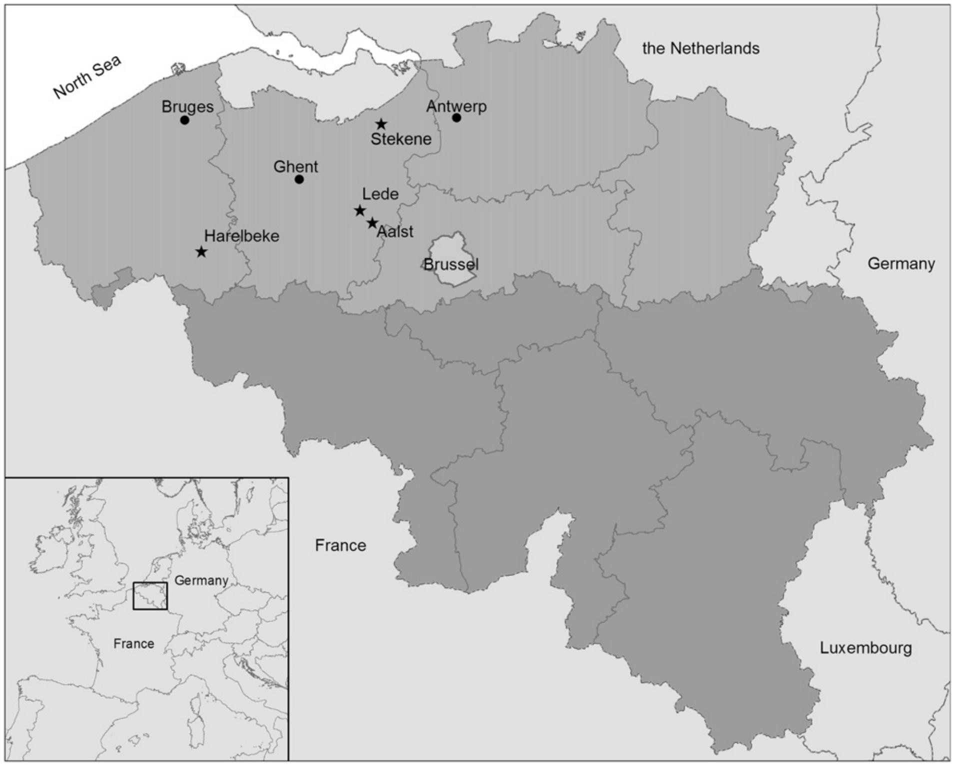

Fig. 2. Location of the selected excavations in Flanders, north-western Belgium.

present in the reconstructed scene. The same low georeferencing errors are also attested in the 3D model of the second dado. This feature was registered with 79 photographs (Fig. 3). The generated point cloud contains 860,000 points and the polygonal mesh contains 14 million faces and 7 million vertices. The georeferencing of the relative model was performed with 30 GCPs and achieved a total RMSE of 0.015 m and 0.008 m, 0.009 m and 0.010 m for the RMSE on the *x*-, *y*- and *z*-coordinates respectively (Table 2).

With this high accuracy, and the possibility to export the 3D model as a 2D orthophoto, the geometric information can be easily integrated in the digital archaeological excavation plan (Fig. 4). If necessary, the archaeological features can be vectorized in a GIS-environment, with an accuracy that is definitely higher than a manual drawing in the field. Fig. 5 shows the (i) the orthophoto generated from the 3D model and (ii) a rectified photograph calculated from one nearly oblique photograph using a 2nd order polynomial transformation. The difference between both solutions clearly shows the remaining positional errors of the latter approach due to the uncorrected lens distortion and topographic displacements. Another advantage of the presented methodology is the possibility to export the model as a DTM. In this way, also height information can be integrated in the digital archaeological excavation plan (Fig. 4). Another added value can be found in the opportunity to calculate the volume of the reconstructed scene. In this case, knowledge of volume of the present bricks per dado is important to quantify the geophysical data from the excavated dadoes and to compare these data with those obtained at non-excavated parts of the Cistercian abbey site.

3.2. A well in the Roman vicus of Harelbeke

Recent development-led excavations, conducted by GATE bvba, revealed a part of the former Roman *vicus* of Harelbeke (Harelbeke, prov. West Flanders, Fig. 2). During these excavations, several wells, providing in a part of the water supply of this Roman settlement, were discovered and investigated (Deconynck and Laloo, 2011). One quadrangular, timber-framed well was selected as a test case for 3D surface modeling. The framework consists of four strong oak cornerposts with horizontally placed planks nailed upon.

The well was documented with 104 photographs using the above described Nikon equipment (Fig. 6). A point cloud of 820,000 points and a polygonal mesh of 9.4 million faces and 4.7 million-vertices were generated with the Agisoft PhotoScan software. The georeferencing of the 3D model was executed with 13 GCPs (Fig. 6). The largest distance between two GCPs measures 4.935 m, while the difference in height between the highest and the lowest GCP is 1.630 m. Again, a very high georeferencing accuracy is attested. The total RMSE measures 0.023 m, while the individual RMSE values for the *x*-, *y*-, and *z*-coordinates attain values of respectively 0.013 m, 0.016 m and 0.011 m (Table 3). Important is not only this high accuracy, but also the high level of surface detail that can be obtained. The holes for the nails, chopping traces in one of the planks and even tree-rings, woodgrains and the structure of the wood are clearly visible (Fig. 6).

3.3. A cellar at the Hopmarkt in Aalst

Since the beginning of the 13th century, the Hopmarkt was located within the city walls of Aalst (Aalst, prov. East Flanders, Fig. 2). In 1497 a Carmelite cloister was founded at this location, which was in use until the French Revolution. After that, the cloister buildings were split up and reused for housing. The development-led excavations at the site were conducted by the public institution SOLVA (De Groote et al., 2011; De Maeyer et al., 2012).

One of the excavated cellars was selected for 3D surface modeling. This cellar was documented with a total of 132 photographs, taken with Olympus μTough-8010 digital camera (Fig. 7). It

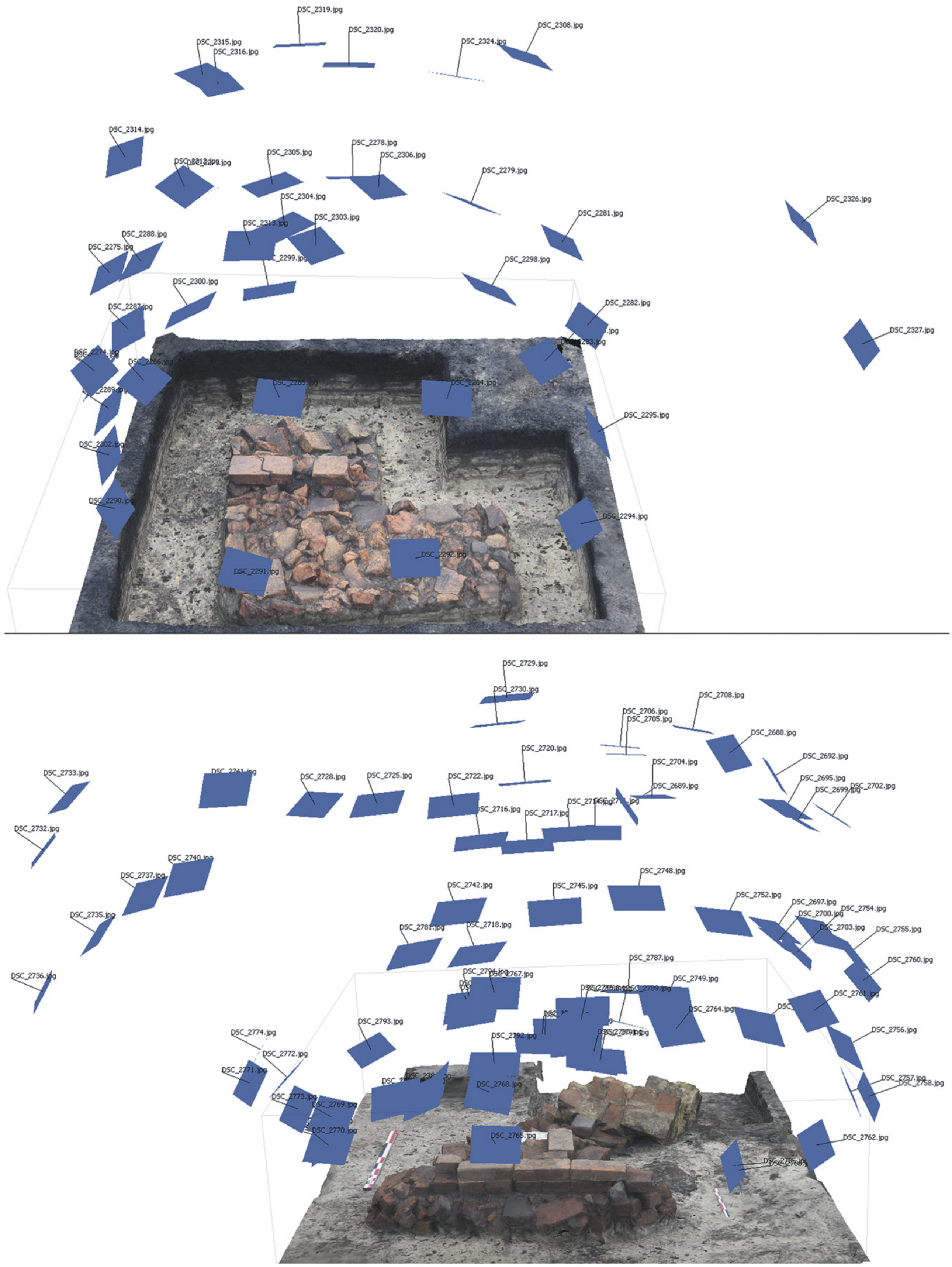

Fig. 3. The textured 3D model with the relative orientation of the camera positions of dado 1 (top) and dado 2 (bottom) on the excavation of the abbey of Boudelo.

Table 1
Georeferencing accuracy of the dado 1 model, with a comparison between the real and estimated *x*-, *y*- and *z*-coordinates (Belgian Lambert 72 coordinates) and the errors (in m) per GCP. The total RMSE and the RMSE for the *x*-, *y*-, and *z*-coordinates are presented at the bottom of the table.

GCP	Real *x*	Real *y*	Real *z*	Est. *x*	Est. *y*	Est. *z*	Error	RMSE (*x*)	RMSE (*y*)	RMSE (*z*)
1	124,004.423	207,565.312	3.288	124,004.416	207,565.305	3.287	0.011	−0.007	−0.007	−0.001
2	124,004.819	207,565.526	3.302	124,004.832	207,565.527	3.293	0.016	0.013	0.001	−0.009
3	124,005.444	207,565.756	3.311	124,005.449	207,565.762	3.284	0.028	0.005	0.006	−0.027
4	124,006.022	207,565.821	3.252	124,006.028	207,565.831	3.255	0.012	0.006	0.010	0.003
5	124,006.166	207,565.376	3.265	124,006.160	207,565.381	3.265	0.008	−0.006	0.005	0.000
6	124,006.261	207,564.890	3.268	124,006.257	207,564.893	3.268	0.005	−0.004	0.003	0.000
7	124,005.683	207,564.586	3.289	124,005.683	207,564.593	3.287	0.007	0.000	0.007	−0.002
8	124,005.791	207,564.011	3.330	124,005.785	207,564.026	3.320	0.019	−0.006	0.015	−0.010
9	124,005.399	207,563.848	3.333	124,005.396	207,563.846	3.329	0.006	−0.003	−0.002	−0.004
10	124,004.930	207,563.677	3.345	124,004.922	207,563.674	3.354	0.012	−0.008	−0.003	0.009
11	124,004.722	207,564.292	3.332	124,004.726	207,564.290	3.332	0.004	0.004	−0.002	0.000
12	124,004.549	207,564.760	3.315	124,004.549	207,564.756	3.319	0.006	0.000	−0.004	0.004
13	124,005.466	207,565.242	3.553	124,005.474	207,565.220	3.576	0.033	0.008	−0.022	0.023
14	124,005.795	207,565.477	3.420	124,005.795	207,565.472	3.435	0.015	0.000	−0.005	0.015
							0.015	**0.006**	**0.009**	**0.011**

need to be noted that the camera positions are not entirely optimized for 3D modeling (i.e. several photographs were taken from the same position). The generated point cloud consists of 580,000 points (Fig. 7) and the polygonal mesh contains 8.5 million faces and 4.2 million vertices. The absolute georeferencing of the resulting 3D model was done using 15 GCPs recorded in the field with a total station. The largest distance between two GCPs measures 6.219 m, while the difference in height between the highest and lowest point is 1.482 m. The georeferencing yielded an absolute total RMSE of 0.009 m while the individual RMSE measured 0.007 m for the *x*-coordinates, 0.005 m for the *y*-coordinates and 0.004 m for the height values (Table 4). Again, this accuracy can never be obtained when manually documenting in the field. Exporting the 3D model as a geometrically correct 2D orthophoto and as a DTM provides again very detailed spatial and height information in the digital excavation plan (Fig. 8).

3.4. Late Medieval horse skeletons

Different from the other sites, the excavations at Lede "Domein Mesen" (Lede, prov. East Flanders, Fig. 2) on terrains nearby the former Medieval castle of Lede, were already conducted in the summer of 2009 (Clement et al., 2012). The excavation, executed by the public institution SOLVA, revealed two horse skeletons next to Iron Age and Roman Age settlement traces and burials, a Medieval settlement with arts and crafts zone and outhouses of the castle of Lede. Both skeletons were dated, based on the associated pottery, to the 14th–16th century AD.

Table 2
Georeferencing accuracy of the dado 2 model, with a comparison between the real and estimated *x*-, *y*- and *z*-coordinates (Belgian Lambert 72 coordinates) and the errors (in m) per GCP. The total RMSE and the RMSE for the *x*-, *y*-, and *z*-coordinates are presented at the bottom of the table.

GCP	Real *x*	Real *y*	Real *z*	Est. *x*	Est. *y*	Est. *z*	Error	RMSE (*x*)	RMSE (*y*)	RMSE (*z*)
1	124,004.612	207,568.796	3.325	124,004.596	207,568.800	3.309	0.022	−0.016	0.004	−0.016
2	124,004.251	207,568.845	3.351	124,004.265	207,568.826	3.323	0.037	0.014	−0.019	−0.028
3	124,004.030	207,568.370	3.298	124,004.028	207,568.364	3.297	0.007	−0.002	−0.006	−0.001
4	124,004.402	207,568.348	3.318	124,004.411	207,568.331	3.307	0.022	0.009	−0.017	−0.011
5	124,004.701	207,568.442	3.317	124,004.685	207,568.449	3.323	0.018	−0.016	0.007	0.006
6	124,004.883	207,568.179	3.303	124,004.875	207,568.171	3.323	0.022	−0.008	−0.008	0.020
7	124,005.162	207,568.220	3.322	124,005.155	207,568.213	3.327	0.011	−0.007	−0.007	0.005
8	124,005.611	207,568.288	3.192	124,005.615	207,568.302	3.193	0.015	0.004	0.014	0.001
9	124,005.482	207,568.777	3.230	124,005.485	207,568.788	3.238	0.014	0.003	0.011	0.008
10	124,005.735	207,568.806	3.234	124,005.743	207,568.814	3.229	0.013	0.008	0.008	−0.005
11	124,005.460	207,569.126	3.253	124,005.454	207,569.131	3.261	0.011	−0.006	0.005	0.008
12	124,005.589	207,569.390	3.243	124,005.585	207,569.409	3.235	0.021	−0.004	0.019	−0.008
13	124,005.044	207,569.570	3.328	124,005.045	207,569.566	3.334	0.007	0.001	−0.004	0.006
14	124,004.822	207,569.637	3.336	124,004.822	207,569.626	3.333	0.012	0.000	−0.011	−0.003
15	124,005.274	207,569.775	3.297	124,005.273	207,569.783	3.306	0.012	−0.001	0.008	0.009
16	124,005.088	207,570.148	3.300	124,005.093	207,570.160	3.306	0.014	0.005	0.012	0.006
17	124,004.762	207,570.093	3.332	124,004.762	207,570.085	3.323	0.012	0.000	−0.008	−0.009
18	124,004.373	207,569.907	3.345	124,004.386	207,569.901	3.335	0.017	0.013	−0.006	−0.010
19	124,004.193	207,569.945	3.343	124,004.193	207,569.942	3.337	0.007	0.000	−0.003	−0.006
20	124,004.367	207,570.267	3.335	124,004.381	207,570.272	3.323	0.019	0.014	0.005	−0.012
21	124,003.960	207,570.420	3.321	124,003.973	207,570.409	3.334	0.022	0.013	−0.011	0.013
22	124,003.581	207,570.383	3.337	124,003.585	207,570.377	3.343	0.010	0.004	−0.006	0.006
23	124,003.278	207,570.106	3.362	124,003.282	207,570.097	3.371	0.013	0.004	−0.009	0.009
24	124,003.045	207,569.882	3.382	124,003.040	207,569.885	3.387	0.008	−0.005	0.003	0.005
25	124,003.114	207,569.478	3.374	124,003.101	207,569.476	3.371	0.013	−0.013	−0.002	−0.003
26	124,003.110	207,569.013	3.354	124,003.105	207,569.021	3.353	0.009	−0.005	0.008	−0.001
27	124,003.176	207,568.471	3.352	124,003.172	207,568.477	3.350	0.008	−0.004	0.006	−0.002
28	124,003.569	207,568.404	3.333	124,003.565	207,568.413	3.336	0.011	−0.004	0.009	0.003
29	124,003.425	207,568.125	3.326	124,003.422	207,568.122	3.336	0.011	−0.003	−0.003	0.010
30	124,003.843	207,568.133	3.304	124,003.847	207,568.132	3.304	0.004	0.004	−0.001	0.000
							0.015	**0.008**	**0.009**	**0.010**

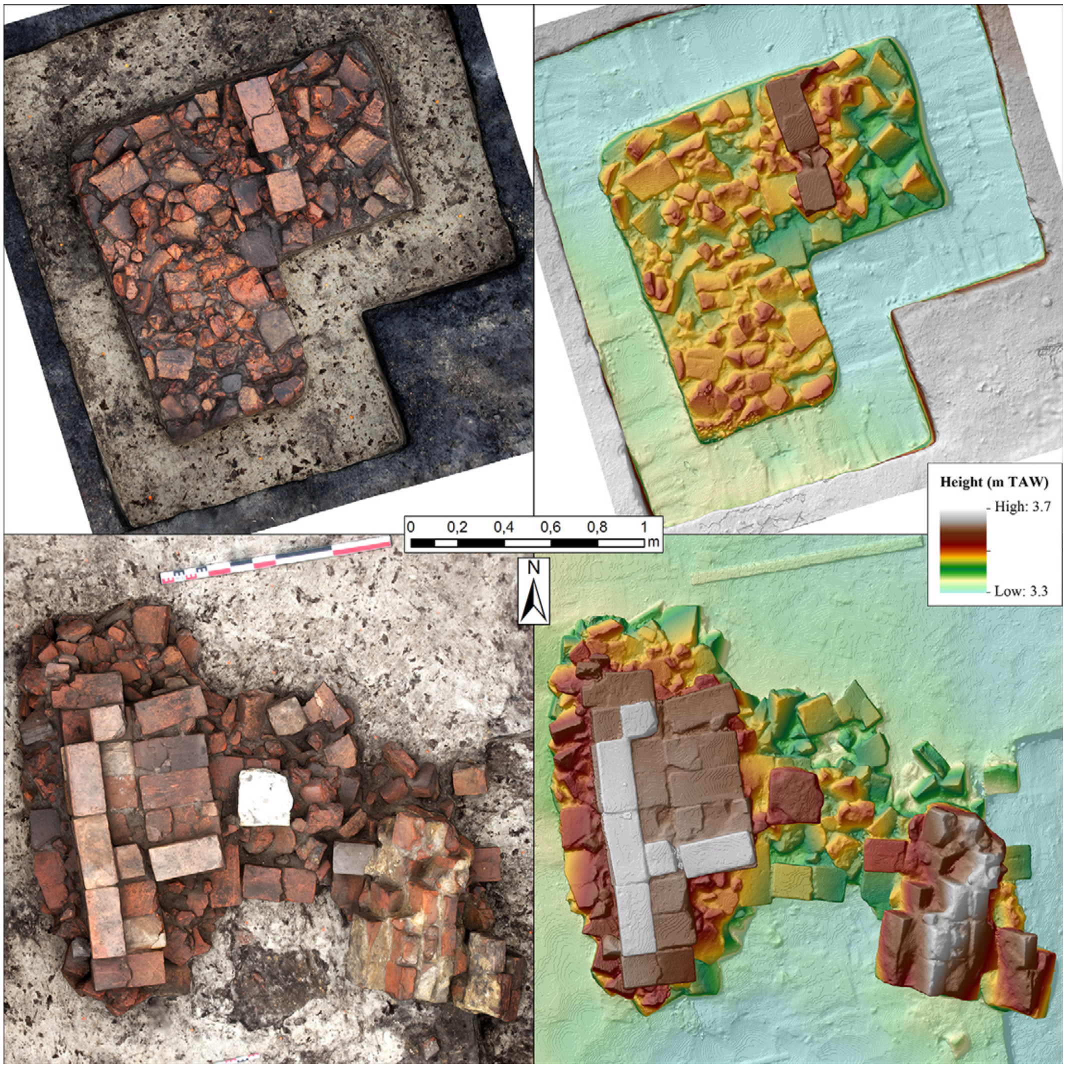

Fig. 4. Orthophoto (left) and DTM (right) generated from the 3D surface model of the two documented dadoes on the excavation of the abbey of Boudelo. The accurate geometric information can easily be integrated in the digital archaeological excavation plan.

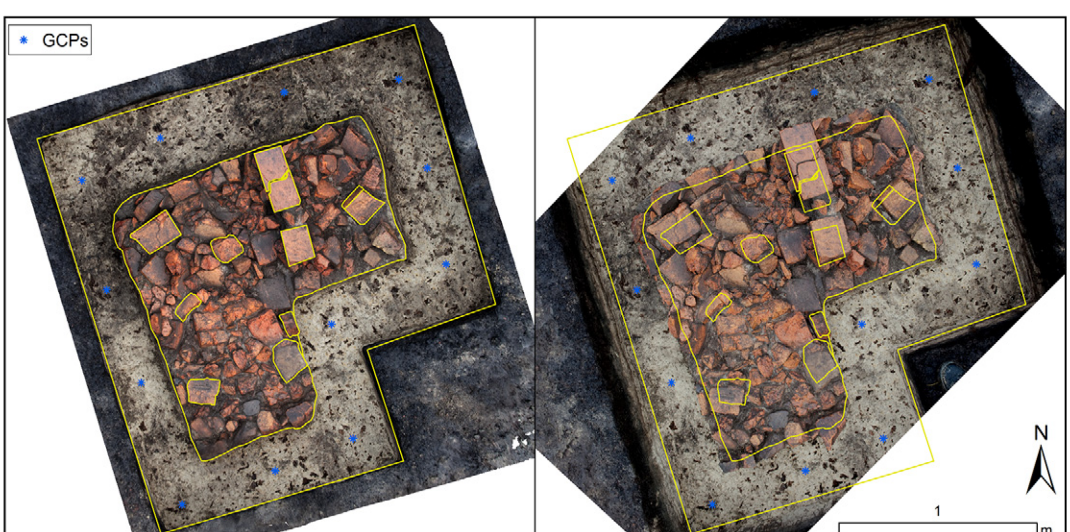

Fig. 5. Comparing the generated orthophoto of the 3D model of dado 1 (left), with a rectified photograph calculated from one nearly oblique photograph using a 2nd order polynomial transformation (right). The figure illustrates the lens distortion and topographic displacements that are remaining in the output of the latter method.

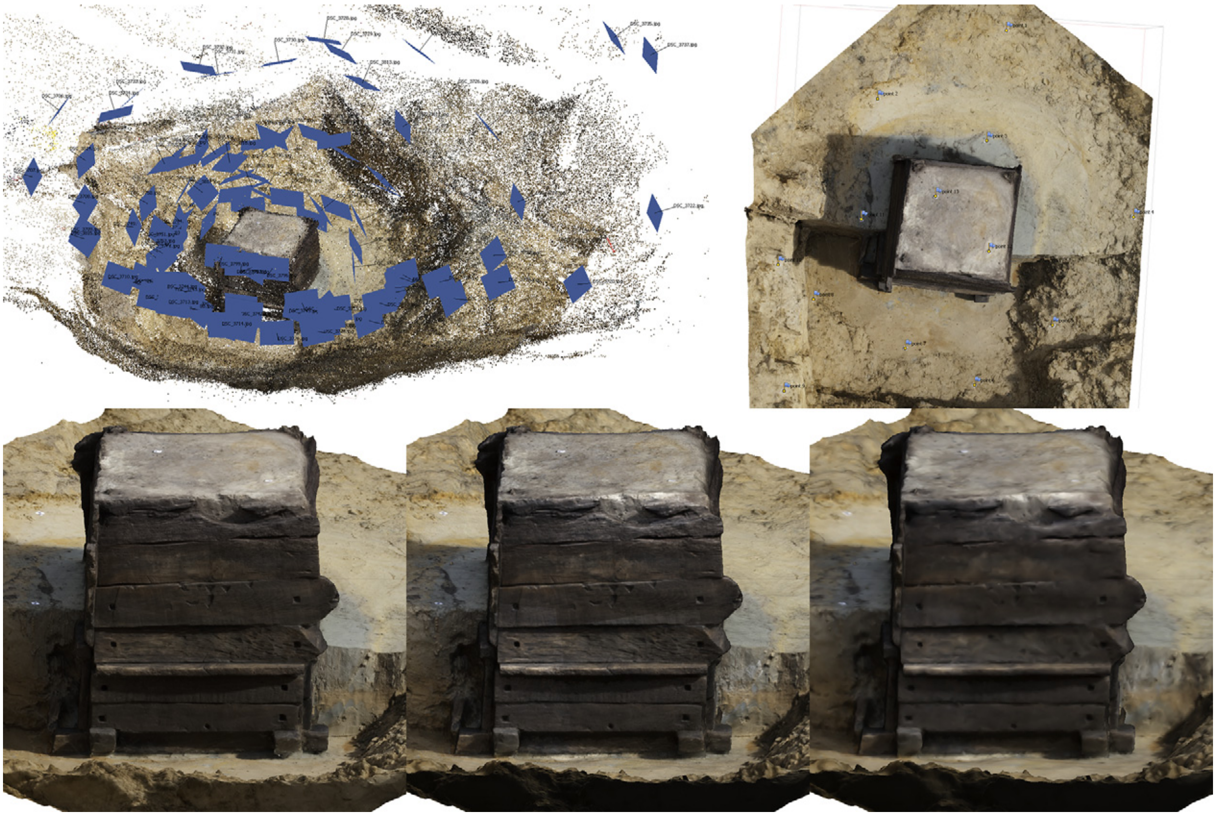

Fig. 6. The Roman well at Harelbeke: 3D sparse point cloud with the relative orientation of the camera positions (top left); orthophoto of the scene with the 13 GCPs (top right); the well as seen from southern direction (bottom), showing the very detailed textured 3D model (bottom left), the polygonal mesh in solid mode (bottom middle) and a decimated polygonal mesh (200,000 faces) in solid mode (bottom right).

The horse skeletons were selected to investigate the possibilities to generate a 3D model out of photographs from “old” excavations that were not intended for 3D modeling. The image overlap and camera positions are far from optimized for a 3D surface reconstruction (Fig. 9). Also no GCPs were recorded. The 24 images available were taken with a Olympus μ-1030 SW digital camera. The generated point cloud consists of 160,000 points, while the polygonal mesh contains 14.8 million faces and 7.4 million vertices. By absence of GCPs, the 3D model cannot be georeferenced. However, the presence of a scale bar next to the skeletons, which can be used as reference distance, allows the scaling of the model and the extraction of metric information concerning the scene. However, more important is the possibility to integrate this detailed textured 3D model in the post-excavation visualization of the archaeological heritage (Fig. 9), e.g. for lectures but also in museums and exhibitions. In the latter case, it allows the public to discover the archaeological heritage for themselves. An archaeological context that can be intriguing for the general public (i.e. two horse skeletons), will even attract attention to the larger archaeological site and to the archaeological heritage sensu stricto when the results are presented with such detailed 3D visualizations.

4. Discussion

Excavating the archaeological heritage is most often a destructive process, especially when no stone structures are preserved or

Table 3
Georeferencing accuracy of the 3D well model, with a comparison between the real and estimated *x*-, *y*- and *z*-coordinates (Belgian Lambert 72 coordinates) and the errors (in m) per GCP. The total RMSE and the RMSE for the *x*-, *y*-, and *z*-coordinates are presented at the bottom of the table.

GCP	Real *x*	Real *y*	Real *z*	Est. *x*	Est. *y*	Est. *z*	Error	RMSE (*x*)	RMSE (*y*)	RMSE (*z*)
1	75,187.472	170,767.599	13.537	75,187.482	170,767.586	13.540	0.017	0.010	−0.013	0.003
2	75,185.818	170,767.296	13.564	75,185.809	170,767.319	13.556	0.026	−0.009	0.023	−0.008
3	75,186.869	170,766.477	13.411	75,186.868	170,766.466	13.410	0.011	−0.001	−0.011	−0.001
4	75,188.194	170,765.105	13.440	75,188.186	170,765.101	13.430	0.014	−0.008	−0.004	−0.010
5	75,186.922	170,764.232	13.007	75,186.956	170,764.238	13.024	0.038	0.034	0.006	0.017
6	75,185.900	170,763.870	12.784	75,185.905	170,763.883	12.803	0.024	0.005	0.013	0.019
7	75,185.288	170,764.511	12.782	75,185.293	170,764.537	12.779	0.027	0.005	0.026	−0.003
8	75,184.489	170,765.390	12.822	75,184.465	170,765.405	12.825	0.029	−0.024	0.015	0.003
9	75,183.633	170,764.498	13.893	75,183.636	170,764.487	13.892	0.011	0.003	−0.011	−0.001
10	75,184.060	170,765.872	13.819	75,184.055	170,765.878	13.829	0.013	−0.005	0.006	0.010
11	75,185.200	170,766.096	13.492	75,185.192	170,766.074	13.471	0.032	−0.008	−0.022	−0.021
12	75,186.329	170,765.253	14.412	75,186.327	170,765.229	14.409	0.024	−0.002	−0.024	−0.003
13	75,185.953	170,766.026	14.382	75,185.954	170,766.022	14.376	0.007	0.001	−0.004	−0.006
							0.023	**0.013**	**0.016**	**0.011**

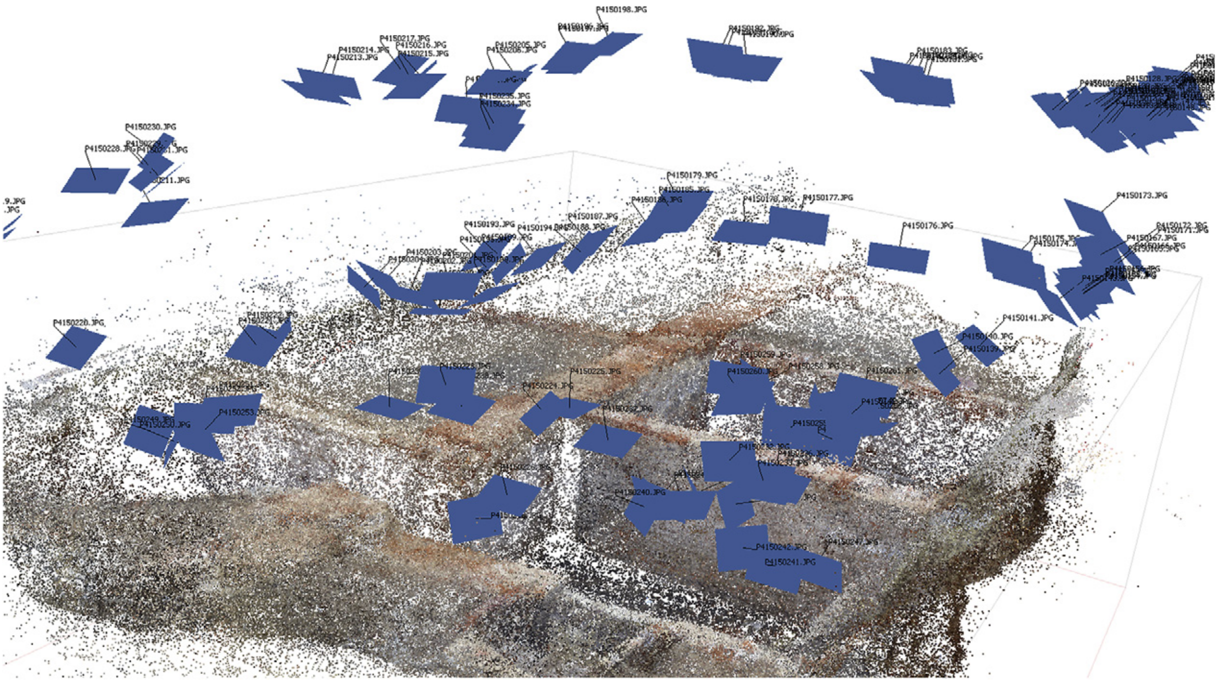

Fig. 7. The cellar at the excavation in Aalst: 3D sparse point cloud with the relative orientation of the camera positions.

when no in-situ preservation for stone structures will follow it. No matter whether these operations are programmed or development-led, an archaeological excavation should aim at a maximal documentation of the site, including a thorough registration and interpretation of every archaeological context. Therefore, archaeological investigations inquire detailed, high-resolution registration and documentation techniques. In this framework, the generation of 3D textured surface models using low-cost computer vision software and standard consumer-grade digital cameras offers opportunities for the extraction of 3D information from photographs and an accurate 3D registration of the archaeological heritage.

A major advantage of the presented methodology and the software package used is the straightforwardness to process the photographs and compute the 3D results. In contrast with traditional photogrammetry or terrestrial laser scanning, it can be executed by any archaeologist, even without a solid technical background in 3D technology. Moreover, no special equipment is needed to generate proper 3D models. Except for the low-cost software package, only standard excavation equipment is needed, including a digital camera to take the photographs, a GPS or total station to record the GCPs and a computer to process the 3D model. Although the processing of a 3D model can be done on a standard computer (dual-core processor, 2 GB RAM and a 32-bit operating system) a more powerful configuration with a multi-core processor, 8–12 GB RAM, a 64-bit operating system and a high-end graphical card are strongly recommended (AgiSoft LLC, 2011a; Doneus et al., 2011). The combination of low-costs and a high accuracy makes the method an efficient and valuable improvement for the registration of the archaeological heritage.

The documentation in the field of an archaeological context for 3D surface modeling can be done fast and efficiently. To generate an accurate and metric 3D model, one only needs (i) a collection of sharp, high-quality photographs covering the context (whereby

Table 4
Georeferencing accuracy of the 3D cellar model, with a comparison between the real and estimated *x*-, *y*- and *z*-coordinates (local coordinates) and the errors (in m) per GCP. The total RMSE and the RMSE for the *x*-, *y*-, and *z*-coordinates are presented at the bottom of the table.

GCP	Real *x*	Real *y*	Real *z*	Est. *x*	Est. *y*	Est. *z*	Error	RMSE (*x*)	RMSE (*y*)	RMSE (*z*)
1	−4.560	7.684	−0.227	−4.554	7.683	−0.222	0.007	0.006	−0.001	0.005
2	−4.279	3.975	−0.229	−4.270	3.968	−0.229	0.011	0.009	−0.007	0.000
3	−3.151	8.404	−0.116	−3.148	8.407	−0.119	0.005	0.003	0.003	−0.003
4	−3.236	6.492	−0.165	−3.234	6.497	−0.170	0.007	0.002	0.005	−0.005
5	−2.985	4.616	−0.136	−2.982	4.617	−0.139	0.004	0.003	0.001	−0.003
6	−2.303	5.401	−0.089	−2.299	5.405	−0.093	0.007	0.004	0.004	−0.004
7	−0.462	5.466	−0.092	−0.466	5.465	−0.092	0.004	−0.004	−0.001	0.000
8	−3.682	3.350	−1.540	−3.679	3.341	−1.539	0.010	0.003	−0.009	0.001
9	−2.085	3.795	−1.460	−2.094	3.792	−1.462	0.010	−0.009	−0.003	−0.002
10	−1.620	5.014	−1.466	−1.632	5.020	−1.463	0.014	−0.012	0.006	0.003
11	−0.088	3.624	−1.401	−0.092	3.621	−1.396	0.007	−0.004	−0.003	0.005
12	−0.494	6.359	−1.571	−0.483	6.358	−1.571	0.011	0.011	−0.001	0.000
13	−2.357	8.196	−1.534	−2.364	8.203	−1.543	0.014	−0.007	0.007	−0.009
14	−0.527	8.709	−0.218	−0.523	8.704	−0.211	0.009	0.004	−0.005	0.007
15	−0.970	8.098	−1.126	−0.978	8.101	−1.120	0.011	−0.008	0.003	0.006
							0.009	**0.007**	**0.005**	**0.004**

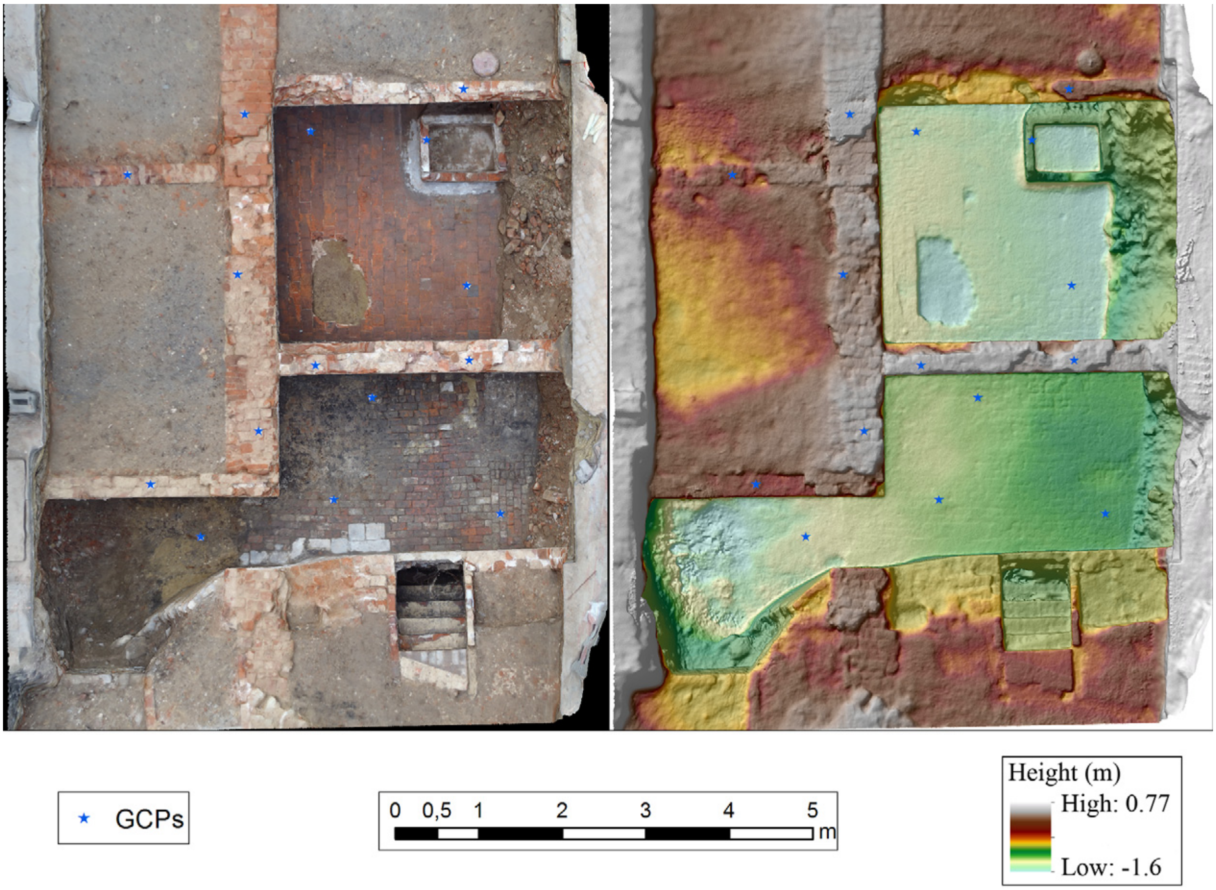

Fig. 8. Orthophoto and DTM generated from the 3D surface model of the documented cellar at the excavation in Aalst, allowing the integration of accurate geometric information in the digital archaeological excavation plan.

each photo is taken from a unique location and with sufficient overlap) and (ii) at least three ground control points. Approximately 15–30 min of fieldwork were required to document a more complex archaeological context (e.g. well, dado or cellar), where traditionally several hours would be required to manually document (e.g. taking tape measurements and drawing) the context. This is a significant time-efficient improvement of the field registration method. Moreover, the possibility to export the 3D model as an orthophoto or a DTM, or the possibility to export the models as a VRML or COLLADA file and import them in a 3D GIS-environment (Opitz and Nowlin, 2012), makes it feasible to integrate detailed and accurate information in the digital archaeological excavation plan.

The traditional manual recording of archeological remains requires an interpretation done by the archaeologist producing the drawing. This interpretation is of fundamental importance for the full understanding of the site during and after the excavation process. As a result of the fast documenting during the fieldwork by using photographs and 3D modeling, there is a certain risk that the process of interpretation is postponed and only happens at a later post-excavation stage, at some remove of the remains and potentially without the possibility to re-engage with the archaeological remains. Such situations must be avoided and the interpretation of the remains should primarily happen during the fieldwork. Moreover, better 3D models will be obtained by firstly interpreting the remains and then optimizing the photographing and documentation strategy to capture all important details. Furthermore, additional information which is not fully rendered in a photograph, such as soil texture, but which can hold important archaeological information still needs to be recorded manually in the field. Apart from this, 3D documentation of archaeological remains provides a more objective and less interpretative view than the traditional manual approach, which is more subjective and is already an interpretation given by the archaeologists. A more objective approach needs to be pursued as it allows future archaeologists to review and reinvestigate the excavation. In addition, the documentation and recording of texture is important for archaeological research as it stores information about colors and appearances of the archaeological remains in an objective way. It is also important to record the paradata of the recording-documentation-interpretation-3D modeling process so that future viewers of the model know exactly how it was recorded and made (Beacham, 2012).

Another advantage of the 3D documenting compared to the traditional literary accounts and graphical depictions is the recording of shape. By using GCPs the shape of the archaeological entity can be recorded and geometrically modeled. By recording shape, variations in shape, which hold important information about the function of objects and spaces in ancient times, are also recorded. Among the analytic possibilities are for example the production of cross-sections, the calculation of volumes and the (comparative) study of size, height, depth and other metrics. To investigate and quantify shape and variations in shape, precise and reliable 3D models are necessary. Therefore, it is important that the software enables the output of highly accurate 3D models with abundant detail, as shown by the presented examples. The high accuracy output of the software has been investigated and described more rigorously by Doneus et al. (2011) and Verhoeven

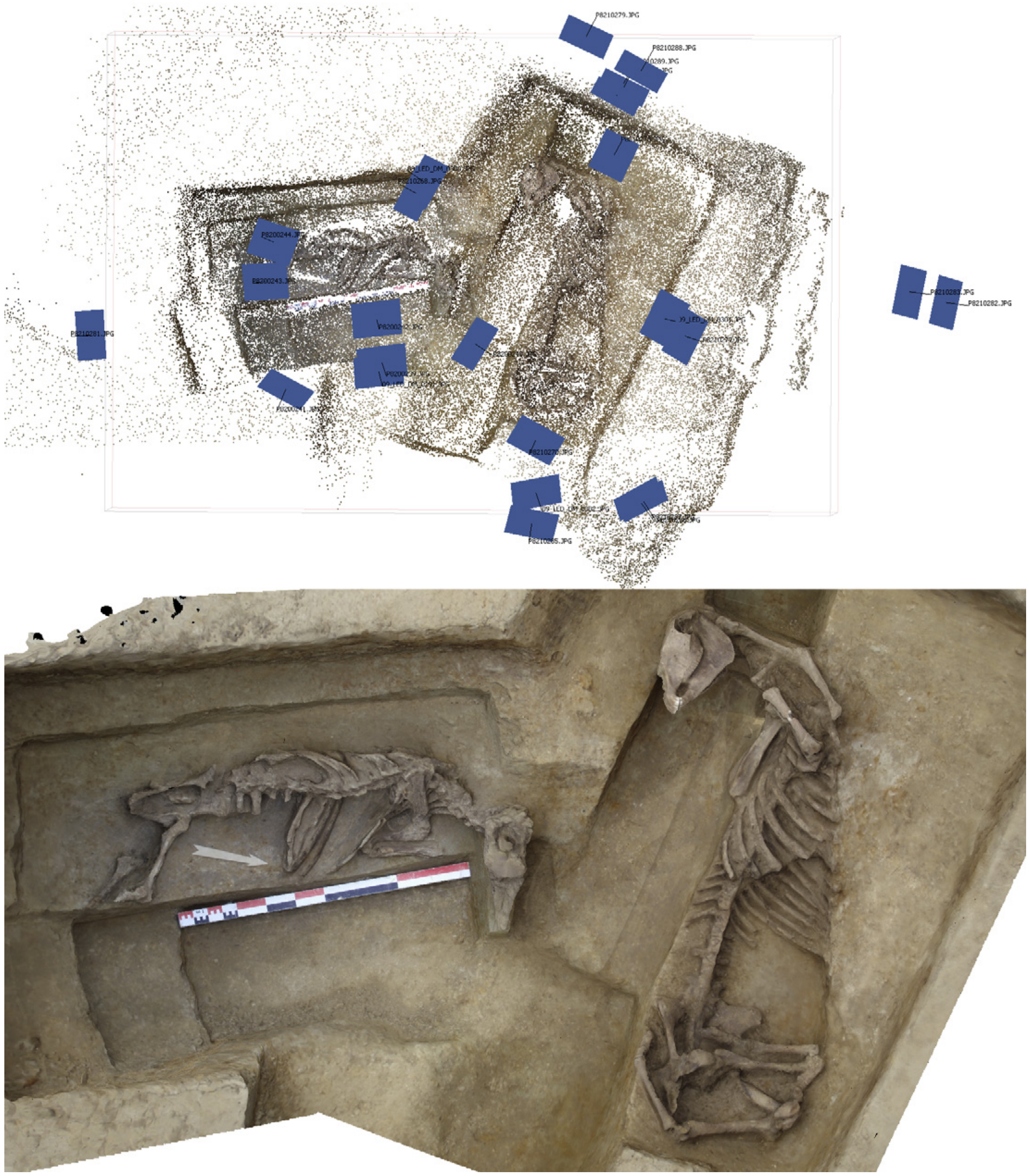

Fig. 9. The Late Medieval horse skeletons: 3D sparse point cloud with the relative orientation of the camera positions (top); mapped texture on the 3D geometric surface (bottom).

et al. (in press). These studies describe a centimeter accuracy of the software. With this high accuracy, the truthfulness of the results is even higher than needed for most archaeological excavations and thus will not change the understanding and interpretation of the archaeological heritage. Nevertheless, archaeologists should aim at documenting an excavation as accurate and detailed as reasonably possible, in particular as it is a destructive process. Therefore, the recording of both the 3D shape and the texture of the archaeological remains is of paramount importance in archaeological research as it aims at a complete and realistic recording and documenting of the archaeology in an objective way. 3D remains are recorded as 3D shape.

Besides its scientific value, 3D documentation of archaeological excavations also has an important communicative and educational value. In particular the visual character of the 3D surface modeling offers possibilities to attract the attention of the general public to the archaeological excavation and archaeological heritage. Where an excavation plan is most often only readable and understandable for the archaeologist, a 3D model is more visible and perceptible for the general public, or as described by Hermon (2008) "*the better the visual tool, the better the explanation and the comprehension of information*". The 3D models can visually support the stories brought by the archaeologist and the public can further discover the heritage themselves by exploring these models. Therefore, of importance is the development of a 3D data dissemination pipeline for post-excavation processing, visualization, exchange and management of the 3D models. A first option is to export the 3D model to an exchangeable PDF format. However, the number of faces needed to be reduced to 200,000 to keep the PDF size within limits and the file manageable (Fig. 6). When decimating the mesh in PhotoScan, the achieved high level of detail is largely lost. This limits the fast exchange of detailed 3D models through PDF. PhotoScan is able to export its data in several file formats without any detail loss (e.g. OBJ). These file formats can be imported in the open source MeshLab software (Visual Computing Group – ISTI – CNR, 2011) that is able to export in the X3D file format that can be viewed by all WebGL/X3DOM enabled web browsers (e.g. Google Chrome, Mozilla Firefox, Opera). However, the export to a XRD file again requires serious decimation. In essence, this is always a problem and the question is also how much details are needed.

Despite the good results, the high accuracy and the straightforward implementation, a number of shortcomings need to be stressed. Intensive and long computation times occur when dealing with large photo collections, high-resolution imagery and/or when a high accuracy is needed. In this trend, large areas (e.g. an entire excavation) are difficult to process in full detail. Furthermore, the PhotoScan software has only been released in 2010 and is still evolving and new versions will appear in the near future to correct possible bugs and errors. Also, alignment errors can occur when only small variations in texture exist or when dealing with highly oblique imagery or with photographs that have dissimilar appearances (Doneus et al., 2011).

5. Conclusion

Despite some shortcomings, mainly computational, the software and the presented methodology proved to be an excellent and suitable method for the 3D registration, documentation and visualization of the excavated archaeological heritage. Especially the "destructive" character of an excavation inquires such registration methods. Advantages can be found in the high accuracy and straightforwardness of the methodology. Compared to the traditional manual registration methods, the improvements of the new methodology have not only an economic, time efficient and cost-effective importance but also a major scientific value. One can proceed from a two-dimensional documentation, often biased by the interpretation of the archaeologist (e.g. drawings), to a multi-dimensional, more objective recording and reproduction of excavated sites that can be used for future studies of the archaeological heritage. This also opens important opportunities towards visualization and participation of the unmovable archaeological heritage in wider than scientific communities.

Acknowledgments

Our appreciation goes to Dr Anestis Koutsoudis and two anonymous referees of *Journal of Archaeological Science* for their helpful and useful comments and suggestions on an earlier version of this paper.

References

AgiSoft LLC, 2011a. AgiSoft PhotoScan User Manual: Standard Edition, Version 0.8.4. AgiSoft LLC.

AgiSoft LLC, 2011b. Agisoft PhotoScan. Professional Edition, Version 0.8.4. http://www.agisoft.ru/products/photoscan/.

Al-kheder, S., Al-shawabkeh, Y., Haala, N., 2009. Developing a documentation system for desert palaces in Jordan using 3D laser scanning and digital photogrammetry. Journal of Archaeological Science 36 (2), 537–546.

Autodesk Inc, 2012. Autodesk 123D Catch. http://www.123dapp.com/catch.

Barazzetti, L., Binda, L., Scaioni, M., Taranto, P., 2011. Photogrammetric survey of complex geometries with low-cost software: application to the 'G1' temple in Myson, Vietnam. Journal of Cultural Heritage 12 (3), 253–262.

Barceló, J.A., De Castro, O., Traver, D., Vicente, O., 2003. A 3D model of an archaeological excavation. In: Doerr, M., Sarris, A. (Eds.), The Digital Heritage of Archaeology. Computer Applications and Quantitative Methods in Archaeology, Proceedings of the 30th Conference, Heraklion, Crete, April 2002. Hellenic Ministry of Culture.

Barceló, J.A., Vicente, O., 2004. Some problems in archaeological excavation 3D modelling. In: Ausserer, K.F., Borner, W., Goriany, M., Karlhuber-Vockl, L. (Eds.), Enter the Past. The e-way into the Four Dimensions of Cultural Heritage. CAA 2003. BAR International Series, vol. 1227. Archaeopress, Oxford, pp. 400–404.

Beacham, R.C., 2012. Defining our terms in heritage visualizations. In: Bentkowska-Kafel, A., Baker, D., Denard, H. (Eds.), Paradata and Transparency in Virtual Heritage. Ashgate, Farnham, pp. 7–11.

Bruno, F., Bruno, S., De Sensi, G., Luchi, M.-L., Mancuso, S., Muzzupappa, M., 2010. From 3D reconstruction to virtual reality: a complete methodology for digital archaeological exhibition. Journal of Cultural Heritage 11 (1), 42–49.

Chandler, J.H., Bryan, P., Fryer, J.G., 2007. The development and application of a simple methodology for recording rock art using consumer-grade digital cameras. The Photogrammetric Record 22 (117), 10–21.

Chandler, J.H., Fryer, J.G., Kniest, H.T., 2005. Non-invasive three-dimensional recording of aboriginal rock art using cost-effective digital photogrammetry. Rock Art Research 22 (2), 119–130.

Chow, S.-K., Chan, K.-L., 2009. Reconstruction of photorealistic 3D model of ceramic artefacts for interactive virtual exhibition. Journal of Cultural Heritage 10 (2), 161–173.

Clarkson, C., Hiscock, P., 2011. Estimating original flake mass from 3D scans of platform area. Journal of Archaeological Science 38 (5), 1062–1068.

Clement, C., Pede, R., Cherretté, B., 2012. Lede Domein Mesen. Archeologisch onderzoek. In: SOLVA Archeologie-Rapport, 11. SOLVA, Aalst.

De Clercq, W., Bats, M., Bourgeois, J., Crombé, P., De Mulder, G., De Reu, J., Herremans, D., Laloo, P., Lombaert, L., Plets, G., Sergant, J., Stichelbaut, B., 2012. Developer-led archaeology in Flanders: an overview of practices and results in the period 1990–2010. In: Webley, L., Vander Linden, M., Haselgrove, C., Bradley, R. (Eds.), Development-led Archaeology in Northwest Europe. Proceedings of a Round Table at the University of Leicester. 19th–21st November 2009. Oxbow Books, Oxford, pp. 29–55.

De Groote, K., De Maeyer, W., Moens, J., Quintelier, K., Van Cleven, F., Vanden Berghe, I., Vernaeve, W., 2011. Het karmelietenklooster van Aalst (prov. Oost-Vl.) (1497–1797): het gebouwenbestand, de begravingen en het fysisch-antropologische onderzoek. Relicta, Archeologie, Monumenten- en Landschapsonderzoek in Vlaanderen 8, 83–250.

De Maeyer, W., Van Cauwenbergh, S., Klinkenborg, S., Taelman, E., Cherretté, B., 2012. Aalst Hopmarkt. Archeologisch onderzoek. In: SOLVA Archeologie-Rapport, 25. SOLVA, Aalst.

De Smedt, P., Van Meirvenne, M., Simpson, D., 2011. Multi-signal EMI and geoarchaeology. Evaluating integrated magnetic susceptibility measurements for archaeological prospection. In: Drahor, M.G., Berge, M.A. (Eds.), Extended Abstracts Archaeological Prospection, 9th International Conference on Archaeological Prospection, September 19 – 24, 2011 Izmir – Turkey.

Deconynck, J., Laloo, P., 2011. Nieuwsbrief 7 archeologische opgraving Harelbeke OCMW: 4 juli – 9 september 2011. Ghent Archaeological Team bvba, Gent.

Doneus, M., Neubauer, W., 2005. 3D laser scanners on archaeological excavations. In: Dequal, S. (Ed.), Proceedings of the XXth International Symposium CIPA, Torino 2005. The International Archives of Photogrammetry, Remote Sensing and Spatial Information Sciences, XXXVI-5/C34/1, pp. 226–231.

Doneus, M., Verhoeven, G., Fera, M., Briese, C., Kucera, M., Neubauer, W., 2011. From deposit to point cloud – a study of low-cost computer vision approaches for the straightforward documentation of archaeological excavations. In: Čepek, A. (Ed.), XXIIIrd International CIPA Symposium, Prague, 12–16 September 2011. Geoinformatics, vol. 6. Faculty of Civil Enginnering, Czech Technical University, Prague, pp. 81–88.

Entwistle, J.A., McCaffrey, K.J.W., Abrahams, P.W., 2009. Three-dimensional (3D) visualisation: the application of terrestrial laser scanning in the investigation of historical Scottish farming townships. Journal of Archaeological Science 36 (3), 860–866.

Eos Systems Inc, 2012. PhotoModeler Scanner. http://www.photomodeler.com/products/pm-scanner.htm.

Fatuzzo, G., Mussumeci, G., Oliveri, S.M., Sequenzia, G., 2011. The "Guerriero di Castiglione": reconstructing missing elements with integrated non-destructive 3D modelling techniques. Journal of Archaeological Science 38 (12), 3533–3540.

Fowles, P.S., Larson, J.H., Dean, C., Solajic, M., 2003. The laser recording and virtual restoration of a wooden sculpture of Buddha. Journal of Cultural Heritage 4 (Suppl. 1 (0)), 367–371.

Grün, A., Remondino, F., Zhang, L., 2004. Photogrammetric reconstruction of the Great Buddha of Bamiyan, Afghanistan. The Photogrammetric Record 19 (107), 177–199.

Guidi, G., Beraldin, J.A., Atzeni, C., 2004. High-accuracy 3D modeling of cultural heritage: the digitizing of Donatello's "Maddalena". Image Processing, IEEE Transactions on 13 (3), 370–380.

Hendrickx, M., Gheyle, W., Bonne, J., Bourgeois, J., De Wulf, A., Goossens, R., 2011. The use of stereoscopic images taken from a microdrone for the documentation of heritage – An example from the Tuekta burial mounds in the Russian Altay. Journal of Archaeological Science 38 (11), 2968–2978.

Hermon, S., 2008. Reasoning in 3D: a critical appraisal of the role of 3D modelling and virtual reconstructions in archaeology. In: Frischer, B., Dakouri-Hild, A. (Eds.), Beyond Illustration: 2D and 3D Digital Technologies as Tools for Discovery in Archaeology. BAR International Series 1805. Archaeopress, Oxford, pp. 35–44.

Karasik, A., Smilansky, U., 2008. 3D scanning technology as a standard archaeological tool for pottery analysis: practice and theory. Journal of Archaeological Science 35 (5), 1148–1168.

Karauğuz, G., Çorumluoğlu, Ö., KalaycI, I., Asri, I., 2009. 3D Photogrammetric model of Eflatunpinar monument at the age of Hittite empire in Anatolia. Journal of Cultural Heritage 10 (2), 269–274.

Katsianis, M., Tsipidis, S., Kotsakis, K., Kousoulakou, A., 2008. A 3D digital workflow for archaeological intra-site research using GIS. Journal of Archaeological Science 35 (3), 655–667.

Koutsoudis, A., Arnaoutoglou, F., Chamzas, C., 2007. On 3D reconstruction of the old city of Xanthi. A minimum budget approach to virtual touring based on photogrammetry. Journal of Cultural Heritage 8 (1), 26–31.
Koutsoudis, A., Chamzas, C., 2011. 3D pottery shape matching using depth map images. Journal of Cultural Heritage 12 (2), 128–133.
Koutsoudis, A., Pavlidis, G., Arnaoutoglou, F., Tsiafakis, D., Chamzas, C., 2009. Qp: a tool for generating 3D models of ancient Greek pottery. Journal of Cultural Heritage 10 (2), 281–295.
Koutsoudis, A., Pavlidis, G., Liami, V., Tsiafakis, D., Chamzas, C., 2010. 3D Pottery content-based retrieval based on pose normalisation and segmentation. Journal of Cultural Heritage 11 (3), 329–338.
Kristiansen, K., 2009. Contract archaeology in Europe: an experiment in diversity. World Archaeology 41 (4), 641–648.
Lambers, K., Eisenbeiss, H., Sauerbier, M., Kupferschmidt, D., Gaisecker, T., Sotoodeh, S., Hanusch, T., 2007. Combining photogrammetry and laser scanning for the recording and modelling of the Late Intermediate Period site of Pinchango Alto, Palpa, Peru. Journal of Archaeological Science 34 (10), 1702–1712.
Lerma, J.L., Navarro, S., Cabrelles, M., Villaverde, V., 2010. Terrestrial laser scanning and close range photogrammetry for 3D archaeological documentation: the Upper Palaeolithic Cave of Parpalló as a case study. Journal of Archaeological Science 37 (3), 499–507.
Lerones, P.M., Fernández, J.L., Gil, Á.M., Gómez-García-Bermejo, J., Casanova, E.Z., 2010. A practical approach to making accurate 3D layouts of interesting cultural heritage sites through digital models. Journal of Cultural Heritage 11 (1), 1–9.
Lin, S.C.H., Douglass, M.J., Holdaway, S.J., Floyd, B., 2010. The application of 3D laser scanning technology to the assessment of ordinal and mechanical cortex quantification in lithic analysis. Journal of Archaeological Science 37 (4), 694–702.
Losier, L.M., Pouliot, J., Fortin, M., 2007. 3D geometrical modeling of excavation units at the archaeological site of tell 'Acharneh (Syria)'. Journal of Archaeological Science 34 (2), 272–288.
McPherron, S.P., Gernat, T., Hublin, J.-J., 2009. Structured light scanning for high-resolution documentation of in situ archaeological finds. Journal of Archaeological Science 36 (1), 19–24.
Microsoft Corporation, 2011. Microsoft Photosynth. http://photosynth.net.
Niven, L., Steele, T.E., Finke, H., Gernat, T., Hublin, J.-J., 2009. Virtual skeletons: using a structured light scanner to create a 3D faunal comparative collection. Journal of Archaeological Science 36 (9), 2018–2023.
Opitz, R., Nowlin, J., 2012. Photogrammetric Modeling + GIS. Better methods for working with mesh data. ArcUser 57, 46–49.
Pavlidis, G., Koutsoudis, A., Arnaoutoglou, F., Tsioukas, V., Chamzas, C., 2007. Methods for 3D digitization of cultural heritage. Journal of Cultural Heritage 8 (1), 93–98.
Plets, G., Gheyle, W., Verhoeven, G., De Reu, J., Bourgeois, J., Verhegge, J., Stichelbaut, B., 2012a. Towards a three-dimensional registration of the archaeological heritage of the Altai Mountains. Antiquity 86 (333), 884–897.
Plets, G., Verhoeven, G., Cheremisin, D., Plets, R., Bourgeois, J., Stichelbaut, B., Gheyle, W., De Reu, J., 2012b. The deteriorating preservation of the Altaian rock art – Assessing three-dimensional image-based modelling in rock art research and management. Rock Art Research 29 (2), 139–156.
Pollefeys, M., Koch, R., Vergauwen, M., Van Gool, L., 2000. Automated reconstruction of 3D scenes from sequences of images. ISPRS Journal of Photogrammetry and Remote Sensing 55 (4), 251–267.
Pollefeys, M., Van Gool, L., Vergauwen, M., Cornelis, K., Verbiest, F., Tops, J., 2003. 3D recording for archaeological fieldwork. Computer Graphics and Applications, IEEE 23 (3), 20–27.
Rajani, M.B., Patra, S.K., Verma, M., 2009. Space observation for generating 3D perspective views and its implication to the study of the archaeological site of Badami in India. Journal of Cultural Heritage 10 (Suppl. 1), 20–26.
Remondino, F., El-Hakim, S., 2006. Image-based 3D modelling: a review. The Photogrammetric Record 21 (115), 269–291.
Remondino, F., Rizzi, A., Girardi, S., Petti, F.M., Avanzini, M., 2010. 3D Ichnology—recovering digital 3D models of dinosaur footprints. The Photogrammetric Record 25 (131), 266–282.
Rua, H., Alvito, P., 2011. Living the past: 3D models, virtual reality and game engines as tools for supporting archaeology and the reconstruction of cultural heritage – the case-study of the Roman villa of Casal de Freiria. Journal of Archaeological Science 38 (12), 3296–3308.
Sanz, J.O., Docampo, M.d.l.L.G., Rodríguez, S.M., Sanmartín, M.T.R., Cameselle, G.M., 2010. A simple methodology for recording petroglyphs using low-cost digital image correlation photogrammetry and consumer-grade digital cameras. Journal of Archaeological Science 37 (12), 3158–3169.
Scharstein, D., Szeliski, R., 2002. A taxonomy and evaluation of dense two-frame stereo correspondence algorithms. International Journal of Computer Vision 47 (1), 7–42.
Seitz, S.M., Curless, B., Diebel, J., Scharstein, D., Szeliski, R., 2006. A comparison and evaluation of multi-view stereo reconstruction algorithms. In: Proceedings of the CVPR '06 IEEE Computer Society Conference on Computer Vision and Pattern Recognition, vol. 1.1. IEEE Computer Society, Washington, DC, pp. 519–528.
Simpson, A., Clogg, P., DÍaz-Andreu, M., Larkman, B., 2004. Towards three-dimensional non-invasive recording of incised rock art. Antiquity 78 (301), 692–698.
Snavely, N., 2010. Bundler: Structure from Motion (SfM) for Unordered Image Collections. http://phototour.cs.washington.edu/bundler/.
Stojakovic, V., Tepavcevic, B., 2011. Image-based modeling approach in creating 3D morphogenetic reconstruction of Liberty Square in Novi Sad. Journal of Cultural Heritage 12 (1), 105–110.
Szeliski, R., 2011. Computer Vision: Algorithms and Applications. Texts in Computer Science. Springer, London.
Tokmakidis, K., Skarlatos, D., 2002. Mapping excavations and archaeological sites using close range photos. In: Proceedings of the ISPRS Commission V Symposium "Close Range Imaging, Long Range Vision", Sep. 2–6 2002, Corfu, Greece.
Tsiafakis, D., Tsirliganis, N., Pavlidis, G., Evangelidis, V., Chamzas, C., 2004. Karabournaki-recording the past: the digitization of an archaeological site. In: International Conference on Electronic Imaging & the Visual Arts EVA 2004, (Florence, Italy), 29 March–2 April 2004. Florence.
Ullman, S., 1979. The interpretation of structure from motion. Proceedings of the Royal Society of London. Series B. Biological Sciences 203 (1153), 405–426.
Verhoeven, G., 2011. Taking computer vision aloft – archaeological three-dimensional reconstructions from aerial photographs with photoscan. Archaeological Prospection 18 (1), 67–73.
Verhoeven, G., Doneus, M., Briese, C., Vermeulen, F., 2012. Mapping by matching: a computer vision-based approach to fast and accurate georeferencing of archaeological aerial photographs. Journal of Archaeological Science 39 (7), 2060–2070.
Verhoeven, G., Taelman, D., Vermeulen, F. Computer vision-based orthophoto mapping of complex archaeological sites: the ancient quarry of Pitaranha (Portugal-Spain). Archaeometry, in press.
VISICS, 2011. ARC 3D Webservice. http://homes.esat.kuleuven.be/~visit3d/webservice/v2/index.php.
Visual Computing Group - ISTI - CNR, 2011. MeshLab. http://meshlab.sourceforge.net/.
Wu, C., 2012. VisualSFM: a Visual Structure from Motion System. http://www.cs.washington.edu/homes/ccwu/vsfm/.
Yastikli, N., 2007. Documentation of cultural heritage using digital photogrammetry and laser scanning. Journal of Cultural Heritage 8 (4), 423–427.
Zapassky, E., Finkelstein, I., Benenson, I., 2006. Ancient standards of volume: negevite Iron Age pottery (Israel) as a case study in 3D modeling. Journal of Archaeological Science 33 (12), 1734–1743.